Highly episodic fire and erosion regime over the past 2,000 y in the Siskiyou Mountains, Oregon

Daniele Colombaroli[a,b,c,1] and Daniel G. Gavin[a]

[a]Department of Geography, University of Oregon, Eugene, OR 97405; and [b]Institute of Plant Sciences and [c]Oeschger Centre for Climate Change Research, University of Bern, CH-3012 Bern, Switzerland

Edited by John P. Smol, Queen's University, Kingston, ON, Canada, and accepted by the Editorial Board September 3, 2010 (received for review June 21, 2010)

Fire is a primary mode of natural disturbance in the forests of the Pacific Northwest. Increased fuel loads following fire suppression and the occurrence of several large and severe fires have led to the perception that in many areas there is a greatly increased risk of high-severity fire compared with presettlement forests. To reconstruct the variability of the fire regime in the Siskiyou Mountains, Oregon, we analyzed a 10-m, 2,000-y sediment core for charcoal, pollen, and sedimentological data. The record reveals a highly episodic pattern of fire in which 77% of the 68 charcoal peaks before Euro-American settlement cluster within nine distinct periods marked by a 15-y mean interval. The 11 largest charcoal peaks are significantly related to decadal-scale drought periods and are followed by pulses of minerogenic sediment suggestive of rapid sediment delivery. After logging in the 1950s, sediment load was increased fourfold compared with that from the most severe presettlement fire. Less severe fires, marked by smaller charcoal peaks and no sediment pulses, are not correlated significantly with drought periods. Pollen indicators of closed forests are consistent with fire-free periods of sufficient length to maintain dense forest and indicate a fire-triggered switch to more open conditions during the Medieval Climatic Anomaly. Our results indicate that over millennia fire was more episodic than revealed by nearby shorter tree-ring records and that recent severe fires have precedents during earlier drought episodes but also that sediment loads resulting from logging and road building have no precedent in earlier fire events.

historical fire | climate variability | ecological resilience | logging | sediment charcoal

Fire plays a key role structuring ecosystems of the floristically diverse Siskiyou and Klamath Mountains of southwest Oregon and Northwest California (1, 2), driving successional pathways (3) and affecting the erosion rate of soils (4, 5). Fire-history data obtained from tree-ring records suggest that before Euro-American settlement forests supported a mixed-severity fire regime characterized by minor amounts of stand-replacing high-severity fire (6–8). Recent decades of fire suppression, logging, and dense regrowth have increased forest density regionally (9), and that increased tree density, along with longer and warmer summers, may be contributing to increased fire size and severity (10, 11). The belief that recent fires, such as the 196,000-ha Biscuit Fire in 2002, were more severe than the historical norm could be used to justify managing fire hazard through thinning or prescribed fire in currently dense stands (12, 13). However, some have questioned whether increased fuels from fire suppression indeed pose an increased risk of severe fire (14, 15) and whether climate may override fuel as a control of fire occurrence and extent (10, 16).

The historical variability of severe fire in the Pacific Northwest remains a subject of debate. Early 20th century accounts and photographs contrast with tree-ring evidence and show a notable proportion of landscapes in dry forest types had been affected recently by severe fire (17–19). Tree-ring fire-scar records, in contrast, are limited by their inability to reconstruct recurrent high-severity fire; long fire-scar records occur only in areas of low-severity fire (20). Tree-ring fire-scar records also are limited by their relatively short temporal depth, rarely extending before A.D. 1600 and into climatic periods that may be analogous to our current climate. Because the rationale for ecological restoration is rooted in an understanding of an historical baseline, a closer examination of the presettlement pattern and severity of fire in the Siskiyou Mountains could help set more realistic restoration target-points (12, 19) and could reveal whether recent fires have been "catastrophic" or just a continuation of burn-severity patterns typical of recent centuries.

Lake-sediment fire-history records place recent trends in fire occurrence into a unique long-term perspective (21, 22). This approach has been used in high-elevation and subalpine forests of the Siskiyou region and revealed a highly variable fire frequency through the Holocene (23). Here we provide a millennial-scale, high-resolution history of middle-elevation forests where there are concerns about unnaturally high fuel loads and altered fire regimes. Few sediment-based studies have evaluated fire severity (i.e., tree mortality and soil impacts), although there is a potential to reconstruct geomorphic responses to severe fire from signatures in colluvial and alluvial sediment (24). In this study we present a paleoecological record of the last 2,000 y of fire, erosion, and vegetation changes in the dry mixed-conifer/broadleaved evergreen zone of the Siskiyou Mountains to examine (*i*) the variability of fire during the climatic changes of the Medieval Climatic Anomaly (MCA; *ca*. A.D. 900–1300) (25) and the Little Ice Age (LIA; *ca.* A.D. 1500–1800) (16), (*ii*) the history of vegetation change and its link to fire, and (*iii*) the impacts of disturbance on soil erosion rates from pre- to postsettlement times.

Results and Discussion

Fire Variability During the Last 2,000 y. Upper Squaw Lake (hereafter "USL," 42°2′ N; 123° 0.9′ W) is a 7.2-ha landslide-dammed basin located at 930 m above sea level in southwestern Oregon (Fig. 1 and Figs. S1–S3). The basin accumulates sediment delivered from adjacent slopes and via Squaw Creek, draining a 40-km^2 watershed with 1,020 m of relief. Ten meters of sediment marked by faint and distinct laminations consisting of silty gyttja and interbedded inorganic turbidites were cored at a water depth of 14.1 m for charcoal, pollen, and other sedimentological analyses. To consider explicitly the short-term changes in the sedimentation rates of the last 2,000 y, we developed an age-depth model using a Bayesian-like approach that incorporates the magnetic susceptibility profile as a proxy of rapidly deposited minerogenic sediment (26, 27), five accelerator mass spectrom-

Author contributions: D.G.G. designed research and provided scientific leadership; D.C. and D.G.G. performed research; D.C. and D.G.G. analyzed data; and D.C. and D.G.G. wrote the paper.

The authors declare no conflict of interest.

This article is a PNAS Direct Submission. J.P.S. is a guest editor invited by the Editorial Board.

Data deposition: The data reported in this paper have been deposited in the Global Charcoal Database (http://www.ncdc.noaa.gov/paleo/impd/gcd.html).

[1]To whom correspondence should be addressed. E-mail: daniele.colombaroli@ips.unibe.ch.

This article contains supporting information online at www.pnas.org/lookup/suppl/doi:10.1073/pnas.1007692107/-/DCSupplemental.

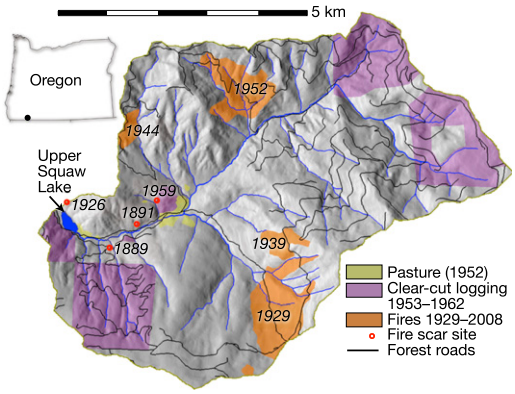

Fig. 1. The location of the 40-km^2 study watershed in southwest Oregon near the California border and a shaded-relief map of the USL watershed, showing extent of pasture and clear-cut logging from 1952 delineated from orthorectified aerial photographs. Fire occurrences are from mapped historical fires and opportunistically sampled fire scars on *Pinus ponderosa*.

etry (AMS) ^{14}C dates on macrofossils, and a determination of the ^{137}Cs peak concentration (Fig. 2 and Fig. S4).

The charcoal stratigraphy, developed at a 2-y mean resolution (1-cm intervals), displays a set of 71 statistically significant peaks (28), which correspond closely with nearby mapped historical fires and tree-ring–dated fire scars (Fig. 2). This clear correspondence indicates that the charcoal record reveals fires that have occurred in at least the lower half of the watershed (Fig. 1 and ref. 29). The 20-y mean fire interval at USL during the period A.D. 1700–1900 also is in broad agreement with nearby tree-ring fire-history studies over the same period (6–8). In contrast with the tree-ring records, the very high sedimentation rate and continuous 2,000-y record at USL makes possible a range of analyses not available to shorter tree-ring records or coarser-resolution sediment records. Specifically, the USL record reveals a highly episodic pattern in which nine distinct fire periods with a 15-y mean interval are separated by periods with a 52-y mean interval (and a maximum interval of 180 y).

The combination of minerogenic sediment pulses and very large peaks in charcoal accumulation suggests that the USL record may record the severity of past fires through their impact on soil stability, revealing severe fire events both recently and in the more distant past. The distribution of charcoal peak sizes supports differentiating the 71 events into a set of 14 large peaks (three of which occur after 1900) and 57 small peaks (Fig. 2 and Fig. S5). The interpretation of the larger charcoal peaks (associated with erosional events) as severe fire is supported by theory and modern calibration studies. These studies have shown that, although charcoal peak size is affected by a combination of fire size, distance from the lake, wind direction, and fire intensity, the charcoal signal resulting from fire intensity is stronger than that for fire proximity or fire extent (29–31). At our site, erosion is an additional but variable contributor of charcoal delivery into the sediment. Based on comparison of charcoal peaks with mapped fires (Fig. 2*F*), the contribution of charcoal coming from more than 3 km upstream is minimal, as shown by other calibration studies (29, 31, 32). Although we cannot place discrete boundaries on the spatial extent of past fires that have contributed to the erosion and fire history, the available evidence suggests the entire USL record is strongly biased toward fires that have occurred in the lower watershed.

The three most recent large charcoal peaks of the 20th century probably were caused primarily by dry-ravel erosion and debris flows following broadcast burning of logging slash in the lower watershed. A fire scar from 1959 adjacent to an area logged in the 1950s confirms the use of fire after logging (Fig. 1). The most recent large charcoal peak postdates this use of fire and is most likely entirely redeposited detrital charcoal resulting from erosion associated with renewed logging in previously burned areas. In contrast, before 20th century land-use impacts, large charcoal peaks slightly precede minerogenic sediment pulses, timing that is consistent with most charcoal being deposited at the time of the fire (not related to erosion), followed by subsoil erosion events (Fig. S6) (33). The minerogenic sediments are marked by low pollen concentrations comprised of high percentages of the species dominating hillslopes (*Pinus* and *Pseudotsuga*) or early successional *Pteridium* (Fig. 3), indicating postfire hillslope erosion.

Overall, this 2,000-y fire history shows that the considerable spatial variation in fire intervals and fire severity observed today in the Siskiyou Mountains also has changed considerably through time. This history is best described as alternations between centennial-scale periods of little to no fire with intervals of frequent fires, probably of small size and low severity, punctuated by larger and/or more severe fires that are associated with distinct erosional signatures. The temporal variability of these events is striking and suggests that, with respect to both fire occurrence and erosional processes, highly nonequilibrium landscapes are typical on centennial time scales.

Climate and Vegetation Controls of the Fire Regime. A comparison of dates of charcoal peaks and a reconstructed drought index [Palmer Drought Severity Index; PDSI (25)] reveals that the most severe fires (largest charcoal peaks) were climate-driven events. Because of the unavoidable uncertainty of the sediment chronology, we examined the climate averaged within a range of window sizes before and after each charcoal peak (Fig. 4). This analysis shows that the 15 y preceding charcoal peaks are marked by significantly lower PDSI than would be expected by chance alone. Lowering the threshold to include smaller charcoal peaks reduced this correlation to marginally significant levels once more than *ca*. 30 fire events were included, as would be expected if the largest or most severe events were most tightly linked to climate. Centennial-scale patterns of fire also were linked to longer-term climate change. Three large charcoal peaks (A.D. 990, 1050, and 1250) occurred during the MCA period, which included widespread and severe periods of drought that are known to have promoted similarly episodic patterns of fire in wetter coastal forests to the north (34). In contrast, during the LIA, distinct charcoal peaks and minerogenic sediments were rare (one large peak at A.D. 1730), and thus any fires occurring at this time were too small to produce a charcoal peak.

The pollen record indicates changes in forest vegetation consistent with the fire history of the past 2,000 y. During a long fire-free period, A.D. 200–550, elevated pollen percentages of the shade-tolerant understory tree *Taxus brevifolia* suggest forests more dense than occur today, although this interpretation should be supported by additional pollen calibration studies. After the year A.D. 900, a decline in *Taxus* occurred during a fire period (yellow bar, Fig. 3) followed immediately by the largest presettlement charcoal peak (A.D. 990) and the simultaneous decline in Cupressaceae (i.e., *Calocedrus*). This shift in the pollen record indicates a regional shift toward more open vegetation (Fig. 3). Following this fire, the pollen of *Arceuthobium,* a parasite of *Pseudotsuga*, increased and remains abundant until present. *Pseudotsuga* pollen was depressed through the remainder of the record, possibly reflecting suppression of this species by *Arceuthobium*. If so, the effects of this parasite are not a novel effect caused by fire suppression and possibly were enhanced by patchy fires in the past (35). From A.D. 950–1450, five large charcoal peaks and erosion events suggest fuel continuity was sufficient to support severe events that synchronize disturbances. Fire was infrequent after A.D. 1450, with the pollen record showing little vegetation change until 20th century land use. The last century shows a loss of shade-tolerant taxa with an increase

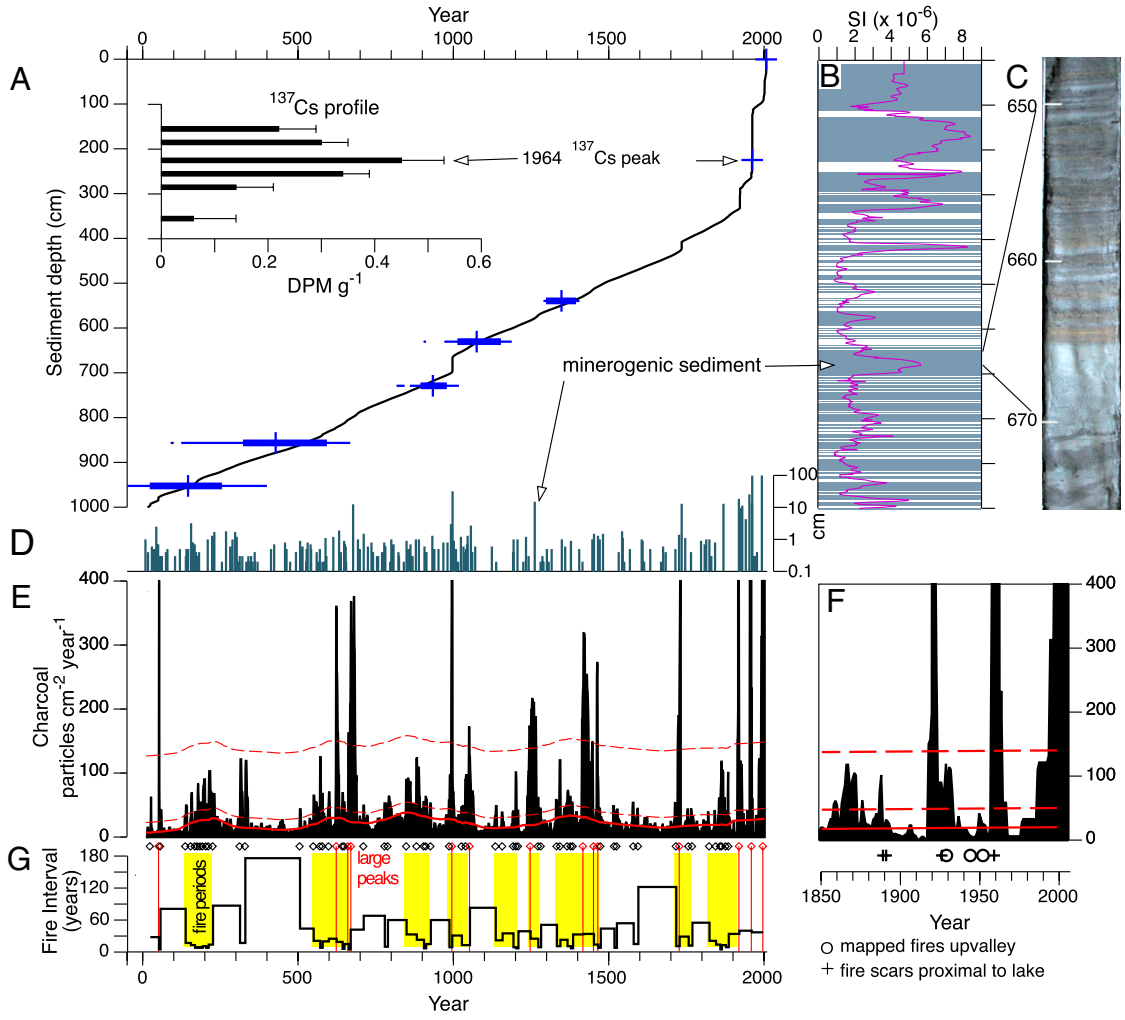

Fig. 2. (*A*) Age–depth model for the USL sediment core. Blue bars indicate calibrated AMS ^{14}C dates, showing 1 and 2 σ age ranges as thick and thin lines, respectively, and median ages as a vertical line. *Inset* shows the ^{137}Cs profile indicating low concentrations and a broad unimodal distribution consistent with rapid sedimentation during the time of the peak ^{137}Cs fallout. The age–depth relationship is based on a model in which bulk sediment magnetic susceptibility is the result of a mixture of rapidly eroded and deposited sediments and slowly deposited organic matter and autochthonous productivity. The model, which accurately fits the ^{14}C and ^{137}Cs dates, is detailed in *Materials and Methods*. (*B*) The magnetic susceptibility profile with depths of visibly light gray sediments indicated by shading. (*C*) A photograph of the core between 648 and 674 cm shows a typical sequence of light gray inorganic sediment followed by banded organic gyttja. (*D*) Thickness of minerogenic sediment from visually detected layers shown in *B*. Most of the thickest layers occur during the past 50 y. (*E*) Charcoal accumulation rate calculated from macroscopic (125–250 μm) charcoal counts in 1- to 3-cm^3 subsamples at 1-cm intervals, expressed as an accumulation rate and interpolated to 2-y intervals. A loess curve fit (solid red line) shows the background above which thresholds are applied at 16 and 120 pieces cm^{-2} y^{-1} (dashed red lines). (*F*) Enlargement of the period 1850–2007 showing raw (noninterpolated) charcoal values. Dates of fires (○) from Forest Service records and fire scars (+) are as shown in Fig. 1. (*G*) Dates of small (black ◊) and large (red ◊) charcoal peaks and fire intervals between observed peaks. Fire periods (yellow background) occurred when there were at least two consecutive intervals of <35 y.

in disturbance-adapted taxa to levels unlike any of the past 2,000 y. The relative stasis of the pollen record before A.D. 1900 indicates that forest ecosystems naturally recovered after fire and drought events, although thresholds in fire severity (such as clearly seen after A.D. 990) may be an important determinant of vegetation shifts.

Despite the general correspondence of fire history with climate and vegetation change, our current understanding of climate and vegetation history is insufficient to explain completely the details of the observed pattern of fire. Refining climate and/or vegetation proxies probably would help explain the episodic pattern of fire at USL. For example, climate-model simulations have shown that the prescription of sea-surface temperature variability affects the spatial patterns of mid-Holocene aridity in the western United States (36). Thus, varying amplitudes of interannual-to-decadal-scale climatic variability (e.g., El Niño Southern Oscillation) could have a major impact on the prevalence of fire climate in our study area (16). Episodic fire patterns also may be promoted by fire–vegetation feedbacks if vegetation switches among alternate stable states (shrublands versus forest) with different levels of pyrogenicity (3). Unfortunately, the open-shrub vegetation types (e.g., *Quercus*) are poorly represented in the USL pollen record and cannot help test this hypothesis.

Comparing Fire and Erosion Before and After A.D. 1900. The USL sediments indicate frequent erosional events throughout the record, but the severe erosion during the 20th century falls outside this historical range of variability. An analysis of the magnitude–frequency distribution of minerogenic horizons for the years A.D. 0–1900 shows a strong fit to a statistical distribution commonly used for flood-frequency analysis (Fig. S7). An extrapolation of this relationship suggests that sedimentation events as large as

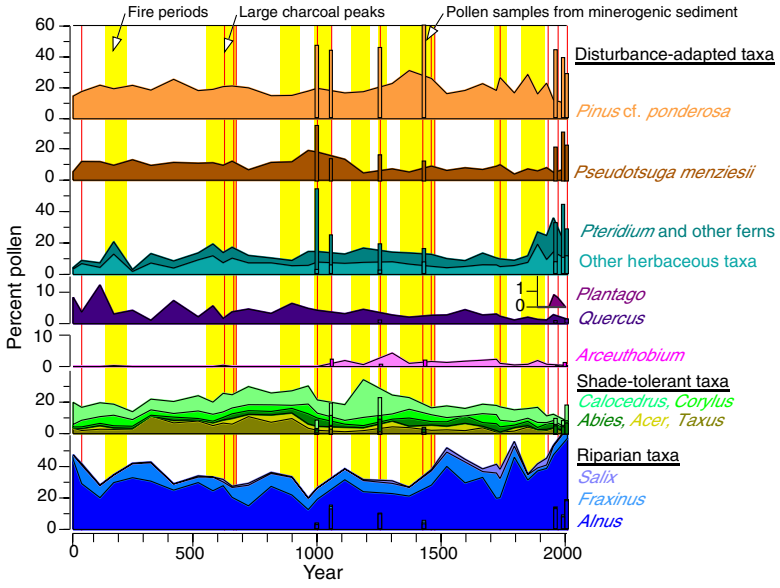

Fig. 3. Summary pollen record showing fire periods (yellow background) and large charcoal peaks (gray lines). Eight pollen samples, shown by vertical bars superimposed on the pollen diagram, are from minerogenic sediment characterized by *ca*. 10-fold lower pollen concentration and high inorganic content and often are associated with large charcoal peaks. The taxon assemblages in these samples are distinctly higher in *Pinus*, *Pseudotsuga*, and fern pollen than are the assemblages from the other samples, consistent with pollen being transported via erosion from hillside soils. Based on the present distribution of species in the area, we assigned *Pinus* subgenus *pinus* to *P. cf ponderosa*, *Pinus* subgenus *Strobus* to *P. cf lambertiana* (not plotted because of low percentages), *Larix*-type to *Pseudotsuga menziesii*, and Cupressaceae to *Calocedrus decurrens*. Note the expanded scales for *Plantago, Quercus* and *Arceuthobium* pollen types.

the events in the 1960s would recur at intervals >10,000 y. Based on the minerogenic sediment thickness and lake bathymetry, we estimate the sediment volume in USL since the 1960s to be 4×10^5 m^3, a volume that corresponds to an average of 15 cm of erosion in the logged areas in the lower watershed. It is likely that the majority of this sediment is derived from roads as well as from isolated debris-flow events (37). Regionally, the interaction of logging activity and heavy rainfall has been found to produce a three- to fourfold increase in sediment load and an orders-of-magnitude increase in the rate of shallow landsliding (37–39), in agreement with the record from USL.

The progression of minerogenic sediment layers reveals that erosion in the 20th century was initiated by land use changes and later exacerbated by several major flood events. The first increase of erosion in the watershed occurred *ca*. 1920, when pollen indicators of disturbance and pasture (*Pteridium* and *Plantago*) increase sharply along with a large charcoal peak and a 30-cm sediment pulse (Fig. 3). This disturbance probably reflects the impact of the homestead at the inlet, where cattle may have directly impacted the banks and channel. After 1952, dense logging road networks were established in two areas (Fig. 1), and the combined effects of the use of tractors to haul logs and the broadcast burning of logging slash further exposed bare soil off-road on steep slopes. Major floods occurred in 1955, 1964, and 1997 following logging and burning. These floods have left geomorphic signatures throughout the region (40), and at USL remnant gullies of debris flows were encountered occasionally in the logged areas.

Conclusions

Our results show clear evidence of a highly episodic and climatically influenced fire regime, with severe fires strongly associated with erosional signatures and decadal-scale droughts. Some periods with very low or almost no fire activity were twice as long as the *ca*. 80 y of fire suppression evident in tree-ring records from the region (6, 7, 18). Therefore the reduction of fire that has occurred since fire suppression began is not qualitatively unusual in the context of the episodic history of fire during the past 2,000 y. The fire regime varied not only on the temporal scales of the LIA and the MCA but also over discrete decadal-scale periods, a pattern which remains mostly unexplained. Therefore we conclude that these landscapes support a non-stationary disturbance regime over a range of time scales.

In contrast to the fire-history record, the sedimentary record from USL indicates that the recent erosion rate falls well outside the historical range of variability. For most of the past 2,000 y, the pollen record shows forests to be naturally resilient, with shade-tolerant species maintaining their abundance even through periods of drought, severe fire, and moderate erosion events. This resiliency was reduced by road building, logging, and major floods. These events resulted in unprecedented dominance by early-successional taxa and a fourfold increase of erosion rates compared with the most severe presettlement fire. The above interpretation suggests that the vegetation and hillslope stability of areas with a legacy of logging and severe erosion will remain sensitive to subsequent severe fire events for the foreseeable future.

The public lands of the Siskiyou region are renowned for being faced with complex fire-management goals for ecological and social objectives (12). To the extent that management is attempting to return forests to their historical conditions, this study suggests that these forests are tolerant of a wide range of fire severity and frequency. However, today's landscapes differ from presettlement landscapes, as shown by the exacerbated erosion rates and modified vegetation of the last 60 y. Returning resiliency to the forested landscape, however achieved, will provide the conditions needed to move into a future with a more fire-conducive climate.

Materials and Methods

Site Description. USL is the smaller of two landslide-dammed basins on Squaw Creek. It is located within the mixed-evergreen and mesic-mixed conifer forest and woodland (Fig. S1). Modern vegetation around the lake consists mainly of *Pseudotsuga menziesii* (Douglas-fir) and smaller amounts of *Arbutus menziesii* (Pacific madrone), *Pinus lambertiana* (sugar pine), *Taxus brevifolia* (Pacific yew), and *Pinus ponderosa* (ponderosa pine), the last with

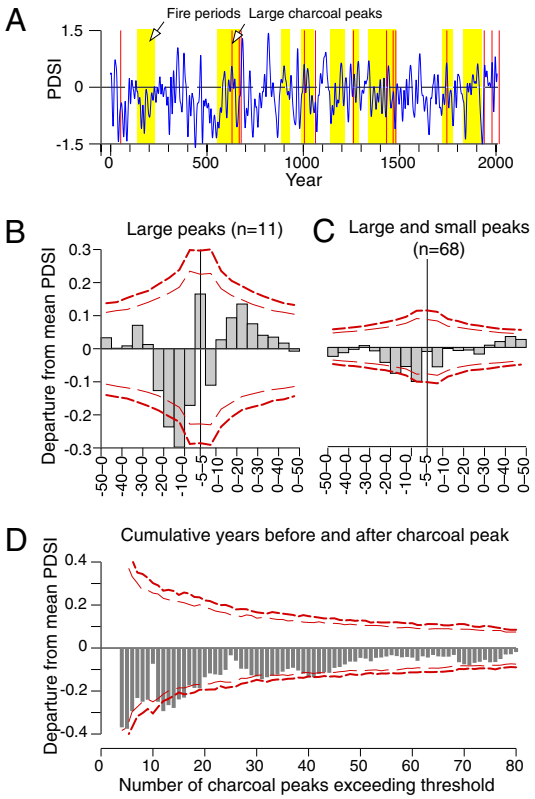

Fig. 4. Reconstruction of drought severity and superposed epoch analysis for charcoal peaks. (*A*) Reconstructed PDSI from four local grid points in Cook (25), smoothed using a 20-y spline. Fire periods are shown as in Fig. 3. (*B* and *C*) Superposed epoch analysis (SEA) (44) showing the mean PDSI preceding, concurrent with, and following charcoal peaks. SEA was modified to address the unknown uncertainty in the sediment chronology. Mean PDSI was calculated in cumulative windows (in 5-y increments) preceding and following the charcoal peaks. The center bar in each plot indicates the period ± 5 y around each charcoal peak. The thin and thick dashed lines show the 90th and 95th percentiles, respectively, based on 5,000 Monte Carlo simulations of charcoal peak years (using a block resampling scheme to preserve the episodic pattern of fire). Analyses did not include fires after A.D. 1900 because of the anthropogenic modification of the fire regime during that period (2, 6). (*D*) SEA applied to a range of fire histories based on continuously varying the peak threshold. SEA was applied for each set of charcoal peaks using only the time window of 15 y preceding the peak. Simulation envelopes were calculated as described above.

fire scars on some of individuals that allowed precise dating of some fire events (Fig. 1). Time series of aerial photographs show that logging commenced shortly after 1952, and these areas now are dominated by *P. menziesii* and *A. menziesii*. The bedrock of 90% of the watershed is graphitic quartz-mica schist and serpentine (41). Climate is characterized by cool, wet winters and hot, dry summers. Precipitation (annual mean 1,100 mm) is concentrated between November and May, so the fire season usually starts in July and lasts until October (8).

Sediment Coring and Chronology. Sediments were retrieved using a 5-cm diameter modified Livingstone piston corer from a raft anchored over the deepest portion of the lake (Fig. S3). Two parallel cores were retrieved in overlapping 1-m drives; basal sediment was not reached. The uppermost 65 cm were sampled using a clear polycarbonate tube fitted with a piston. Cores were returned to the laboratory, split lengthwise, and the overlapping core drives were cross-correlated using multiple visual tie-points to result in an uninterrupted 1,003-cm sediment sequence. Radiocarbon dates were obtained from terrestrial plant macrofossils (Table S1) and calibrated with Calib version 5.0.2. The uppermost samples could not be dated using ^{210}Pb measurements because of a very high sedimentation rate; therefore the 1964 ^{137}Cs peak was located by iterative measurements (Table S2). Distinct banding of minerogenic sediments strongly suggests pulsed fluvial delivery of sediment from hillslope erosion events (33). To account for this cause of variation in sedimentation rate, we used bulk magnetic susceptibility as a proxy of the allochthonous minerogenic component of the lake sediment (26, 33). Magnetic susceptibility (χ) was measured contiguously at 1-cm intervals on the unsplit 5-cm diameter sediment cores using an 8-cm diameter Sapphire Instruments ring meter. The sedimentation rate at each 1-cm depth (S_d) was estimated as a function of the magnetic susceptibility at that depth (χ_d) where χ_d measures the mixture of two end members: (*i*) the autochthonous sediment where $\chi = 0$ and with a sedimentation rate of S_{min} and (*ii*) the instantly deposited allochthonous minerogenic sediment where χ is at or above a critical value (χ_{crit}):

$$S_d = S_{\min} * \chi_{\text{crit}}/(\chi_{\text{crit}} - \chi_d) \text{ for } \chi_d < \chi_{\text{crit}}$$

Although the diamagnetic properties of water, diatoms, and organic matter could result in a negative χ (26), setting S_{min} to a lower χ has very little effect on the model, because the observed χ does not approach 0. The deposition time (y/cm) then is $1/S_d$ or 0 if $\chi_d > \chi_{crit}$, and the sediment age at each depth is the sum of the deposition times above that depth. The model is fit by selecting S_{min} and χ_{crit} to minimize the root mean square error (RMSE) between the model-fit ages and the six age-control points, weighting each control point by its 1σ error estimate (Table S1). The above model resulted in an RMSE of 40 y, underestimating the radiocarbon ages in the lower part of the core. We therefore expanded the two-parameter model to allow S_{min} to change monotonically over the length of the core, resulting in a three-parameter model [i.e., $S_d = (\beta_0+\beta_1 D * \chi_{crit})/(\chi_{crit} - \chi_d)$ where $\beta_0+\beta_1 D$ is the estimate of S_{min} at depth D]. This model yielded an RMSE of only 28 y and was the one chosen for final analysis.

Three other lines of evidence support our interpretation of χ. First, χ_{crit} was fit to a discrete break in the distribution of χ values, separating a distinct population of higher χ (Fig. S4). Second, pollen concentration, biogenic silica concentrations, and loss-on-ignition at depths where $\chi > \chi_{crit}$ are <20% of other samples (Fig. S4). As already mentioned, these pollen assemblages are suggestive of slopewash from subcanopy sites with very high *Pinus* and *Pseudotsuga* and low riparian taxa (Fig. 3). Third, cross-correlation analysis shows that χ peaks by 5–10 y after charcoal (Fig. S6), indicating that high magnetic susceptibility was often the result of fire. Alternative depth–age models that do not consider the magnetic-susceptibility proxy failed to detect periods of higher sedimentation rate (Fig. S8).

Laboratory Analyses. For charcoal analyses, macroscopic charcoal particles were extracted from 1 cm^3 of sediment at contiguous 1-cm intervals and were soaked in a metaphosphate solution and then in a 3% hydrogen peroxide solution for 12 h to remove or lighten the noncharcoal organic content (42). Samples were washed through a 125-μm mesh sieve and counted under a stereomicroscope at a magnification of 40× (30). Particles sieved with a 250-μm mesh sieve showed similar trends similar to the 125-μm fraction, and the two sievings were counted together. Concentrations (particles/cm^3) were converted to charcoal accumulation rates (CHAR, particles cm^{-2} y^{-1}) in 2-y intervals (the median sample deposition time) using CharAnalysis software (28). A slowly varying component of the CHAR, representing secondary charcoal deposition and long-term change in charcoal production (30), was identified by smoothing the influx data with a locally weighted regression robust to outliers (200-y window). The residual series is composed of noise-related variability in CHAR and distinct peaks probably resulting from major fire events. A Gaussian mixture model was used to distinguish the noise component and two other populations (thresholds at 16 and 120 particles cm^{-2} y^{-1}) representing small and large peaks (Fig S5).

To infer past changes in vegetation around the lake, samples every *ca.* 20 cm (corresponding to a mean time resolution of 50 y) for a total of 48 pollen samples were processed following standard procedures (43). A minimum of 300 pollen grains were identified in each sample, except for five samples in which very low pollen concentration occurred because of fast sedimentation rates. These samples clustered closely in age and were combined into single sample with >300 grains for plotting. In total, we counted 61 different pollen types.

ACKNOWLEDGMENTS. We thank C. Bailey, M. Stivers, and E. Bulchis for fieldwork and laboratory assistance, J. van Leeuwen for pollen analyses assistance, and G. Nagle, J. Roering, W. Tinner, P. Bartlein, and two referees for reviewing the manuscript. This project was funded by Swiss National Foundation Fellowship PBBEA 117553 (to D.C.) with additional support from the University of Oregon and the Oeschger Centre for Climate Change Research, University of Bern (Bern, Switzerland).

1. Whittaker RH (1960) Vegetation of the Siskiyou Mountains, Oregon and California. *Ecol Monogr* 30:280–338.
2. Agee JK (1993) *Fire Ecology of Pacific Northwest Forests* (Island, Washington, DC), 493 pp.
3. Odion DC, Moritz MA, DellaSala DA (2010) Alternative community states maintained by fire in the Klamath Mountains, USA. *J Ecol* 98:96–105.
4. Roering JJ, Gerber M (2005) Fire and the evolution of steep, soil-mantled landscapes. *Geology* 33:349–352.
5. Wondzell SM, King JG (2003) Postfire erosional processes in the Pacific Northwest and Rocky Mountain regions. *For Ecol Manage* 178:75–87.
6. Taylor AH, Skinner CN (1998) Fire history and landscape dynamics in a late-successional reserve, Klamath Mountains, California, USA. *For Ecol Manage* 111: 285–301.
7. Taylor AH, Skinner CN (2003) Spatial patterns and controls on historical fire regimes and forest structure in the Klamath Mountains. *Ecol Appl* 13:704–719.
8. Agee JK (1991) Fire history along an elevational gradient in the Siskiyou Mountains, Oregon. *Northwest Sci* 65:188–199.
9. Schoennagel T, Veblen TT, Romme WH (2004) The interaction of fire, fuels, and climate across Rocky Mountain forests. *Bioscience* 54:661–676.
10. Westerling AL, Hidalgo HG, Cayan DR, Swetnam TW (2006) Warming and earlier spring increase western U.S. forest wildfire activity. *Science* 313:940–943.
11. Healey SP, et al. (2008) The relative impact of harvest and fire upon landscape-level dynamics of older forests: Lessons from the Northwest Forest Plan. *Ecosystems* 11: 1106–1119.
12. Dombeck MP, Williams JE, Wood CA (2004) Wildfire policy and public lands: Integrating scientific understanding with social concerns across landscapes. *Conserv Biol* 18:883–889.
13. US Department of Agriculture (2000) *Managing the Impacts of Wildfire on Communities and the Environment: A Report to the President in Response to the Wildfires of 2000* (U.S. Department of Agriculture, Washington). Available at http://www.forest-sandrangelands.gov. Accessed April 28, 2010.
14. Odion DC, Hanson CT (2006) Fire severity in conifer forests of the Sierra Nevada, California. *Ecosystems (N Y)* 9:1177–1189.
15. Hanson CT, Odion DC, DellaSala DA, Baker WL (2009) Overestimation of fire risk in the Northern Spotted Owl recovery plan. *Conserv Biol* 23:1314–1319.
16. Trouet V, Taylor AH, Carleton AM, Skinner CN (2006) Fire-climate interactions in forests of the American Pacific coast. *Geophys Res Lett*, 10.1029/2006GL027502.
17. Leiberg JB (1900) The Cascade Range and Ashland forest reserves and adjacent regions. *USGS Annual Report 21, 1899 -1900* (US Government Printing Office, Washington, DC), Part 5-Forest Reserves, pp 209–498.
18. Beaty RM, Taylor AH (2001) Spatial and temporal variation of fire regimes in a mixed conifer forest landscape, Southern Cascades, California, USA. *J Biogeogr* 28:955–966.
19. Hessburg PF, Salter RB, James KM (2007) Re-examining fire severity relations in pre-management era mixed conifer forests: Inferences from landscape patterns of forest structure. *Landscape Ecol* 22:5–24.
20. Ehle DS, Baker WL (2003) Disturbance and stand dynamics in ponderosa pine forests in Rocky Mountain National Park, USA. *Ecol Monogr* 73:543–566.
21. Willis KJ, Birks HJB (2006) What is natural? The need for a long-term perspective in biodiversity conservation. *Science* 314:1261–1265.
22. Gavin DG, et al. (2007) Forest fire and climate change in western North America: Insights from sediment charcoal records. *Front Ecol Environ* 5:499–506.
23. Briles CE, Whitlock C, Bartlein PJ, Higuera P (2008) Regional and local controls on postglacial vegetation and fire in the Siskiyou Mountains, northern California, USA. *Palaeogeogr Palaeoclimatol Palaeoecol* 265:159–169.
24. Meyer GA, Pierce JL (2003) Climatic controls on fire-induced sediment pulses in Yellowstone National Park and central Idaho: A long-term perspective. *For Ecol Manage* 178:89–104.
25. Cook ER, Woodhouse CA, Eakin CM, Meko DM, Stahle DW (2004) Long-term aridity changes in the western United States. *Science* 306:1015–1018.
26. Thompson R, Battarbee RW, O'Sullivan PE, Oldfield F (1975) Magnetic susceptibility of lake sediments. *Limnol Oceanogr* 20:687–698.
27. Conedera M, et al. (2009) Reconstructing past fire regimes: Methods, applications, and relevance to fire management and conservation. *Quat Sci Rev* 28:435–456.
28. Higuera PE, et al. (2010) Peak detection in sediment-charcoal records: Impacts of alternative data analysis methods on fire-history interpretations. *International Journal of Wildland Fire*, in press.
29. Higuera PE, Peters ME, Brubaker LB, Gavin DG (2007) Understanding the origin and analysis of sediment-charcoal records with a simulation model. *Quat Sci Rev* 26: 1790–1809.
30. Whitlock C, Larsen CPS (2001) Charcoal as a Fire Proxy. *Tracking Environmental Change Using Lake Sediments.* (Kluwer, Dordrecht, The Netherlands), Vol 3, pp 75–97.
31. Duffin KI, Gillson L, Willis KJ (2008) Testing the sensitivity of charcoal as an indicator of fire events in savanna environments: Quantitative predictions of fire proximity, area and intensity. *The Holocene* 18:279–291.
32. Gavin DG, Brubaker LB, Lertzman KP (2003) An 1800-year record of the spatial and temporal distribution of fire from the west coast of Vancouver Island, Canada. *Can J For Res* 33:573–586.
33. Dearing JA (1991) Lake sediment records of erosional processes. *Hydrobiologia* 214: 99–106.
34. Weisberg PJ, Swanson FJ (2003) Regional synchroneity in fire regimes of western Oregon and Washington, USA. *For Ecol Manage* 172:17–28.
35. Shaw DC, Watson DM, Mathiasen RL (2004) Comparison of dwarf mistletoes (*Arceuthobium* spp., Viscaceae) in the western United States with mistletoes (*Amyema* spp., Loranthaceae) in Australia—ecological analogs and reciprocal models for ecosystem management. *Austalian Journal of Botany* 52:481–498.
36. Diffenbaugh NS, Ashfaq M, Shuman B, Williams JW, Bartlein PJ (2006) Summer aridity in the United States: Response to mid-Holocene changes in insolation and sea surface temperature. *Geophys Res Lett*, 10.1029/2006GL028012.
37. Montgomery DR, Schmidt KM, Greenberg HM, Dietrich WE (2000) Forest clearing and regional landsliding. *Geology* 28:311–314.
38. Schmidt KM, et al. (2001) The variability of root cohesion as an influence on shallow landslide susceptibility in the Oregon Coast Range. *Canadian Geotechnical Journal* 38: 995–1024.
39. Sommerfield CK, Drake DE, Wheatcroft RA (2002) Shelf record of climatic changes in flood magnitude and frequency, north-coastal California. *Geology* 30:395–398.
40. Sloan J, Miller JR, Lancaster N (2001) Response and recovery of the Eel River, California, and its tributaries to floods in 1955, 1964, and 1997. *Geomorphology* 36: 129–154.
41. Donato MM (1993) Preliminary geologic map of the Squaw Lakes quadrangle, Oregon and California *Open-File Report OFR 93-703* (US Geological Survey, Reston, VA).
42. Schlachter KJ, Horn SP (2009) Sample preparation methods and replicability in macroscopic charcoal analysis. *J Paleolimnol* 44:701–708.
43. Faegri K, Iversen J (1992) *Textbook of Pollen Analysis* (Hafner, New York).
44. Baisan CH, Swetnam TW (1990) Fire history on a desert mountain range: Rincon Mountain Wilderness, Arizona, USA. *Can J For Res* 20:1559–1569.

Supporting Information

Colombaroli and Gavin 10.1073/pnas.1007692107

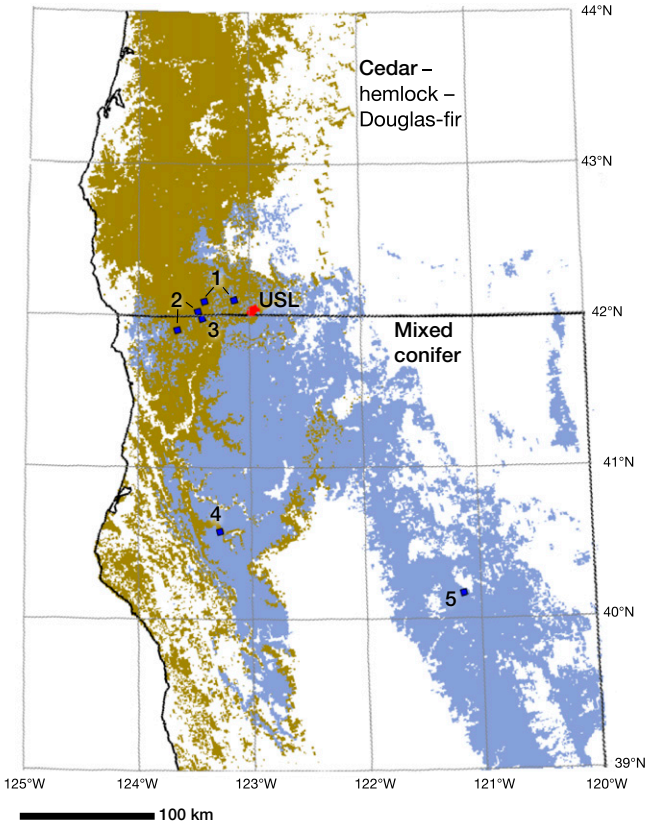

Fig. S1. Regional vegetation and locations of fire-history studies. The study watershed, Upper Squaw Lake (USL), lies near the Oregon–California border. Sites numbered 1 to 5 correspond to the references to fire history studies below. Colors indicate two potential natural vegetation groups (6): cedar–hemlock–Douglas-fir (light yellow) and mixed conifer (blue). Forest vegetation at USL is dominated by *Pseudotsuga menziesii* (Douglas-fir) and *Arbutus menziesii* (Pacific madrone), with *Pinus ponderosa* (ponderosa pine) and *Pinus lambertiana* (sugar pine) also contributing to the canopy on dry slopes. *Quercus chrysolepis* (canyon live oak) is locally abundant on dry slopes as part of the subcanopy. *Fraxinus latifolia* (Oregon ash) and *Alnus rhombifolia* (white alder) dominate the riparian zone. *Quercus garryana* (Oregon white oak) and *Quercus kelloggii* (California black oak) reach their upper-elevation limits near the study site. At elevations >2,000 m, *Abies concolor* (white fir) is more common.

1. Agee JK (1991) Fire history along an elevational gradient in the Siskiyou Mountains, Oregon. *Northwest Sci* 65:188–199.
2. Briles CE, Whitlock C, Bartlein PJ, Higuera P (2008) Regional and local controls on postglacial vegetation and fire in the Siskiyou Mountains, northern California, USA. *Palaeogeography Palaeoclimatology Palaeoecology* 265:159–169.
3. Taylor AH, Skinner CN (1998) Fire history and landscape dynamics in a late-successional reserve, Klamath Mountains, California, USA. *Forest Ecol Manage* 111:285–301.
4. Taylor AH, Skinner CN (2003) Spatial patterns and controls on historical fire regimes and forest structure in the Klamath Mountains. *Ecol Applic* 13:704–719.
5. Beaty RM, Taylor AH (2001) Spatial and temporal variation of fire regimes in a mixed conifer forest landscape, Southern Cascades, California, USA. *J Biogeograph* 28:955–966.
6. Whittaker RH (1960) Vegetation of the Siskiyou Mountains, Oregon and California. *Ecol Monogr* 30:280–338.

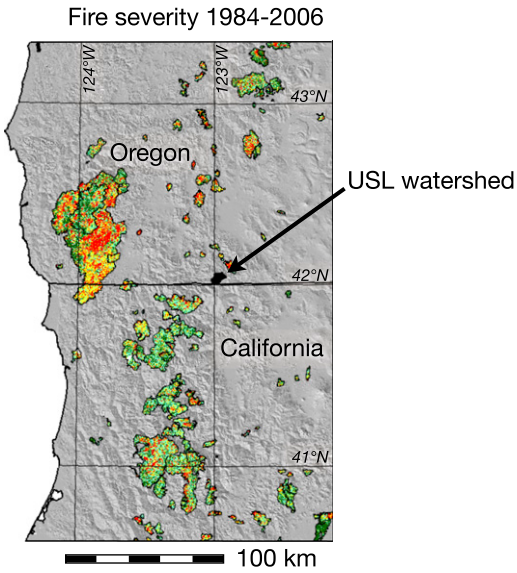

Fig. S2. The severity of fires occurring from 1984 to 2006 in the greater southwest Oregon and northwest California region. Green, yellow, and red indicate low, moderate, and high severity, respectively, determined using the Differenced Normalized Burn Severity Index (1). Data were acquired from the Monitoring Trends in Burn Severity project (2,3).

1. Lutes DC, et al. (2004) *FIREMON: Fire Effects Monitoring and Inventory System* (US Department of Agriculture Forest Service, Rocky Mountain Research Station, Ogden, UT).
2. MTBS, Monitoring Trends in Burn Severity. Available at http://www.mtbs.gov. Accessed December 1, 2009.
3. Eidenshink J, et al. (2007) A project for monitoring trends in burn severity. *Fire Ecol* 3:3–21.

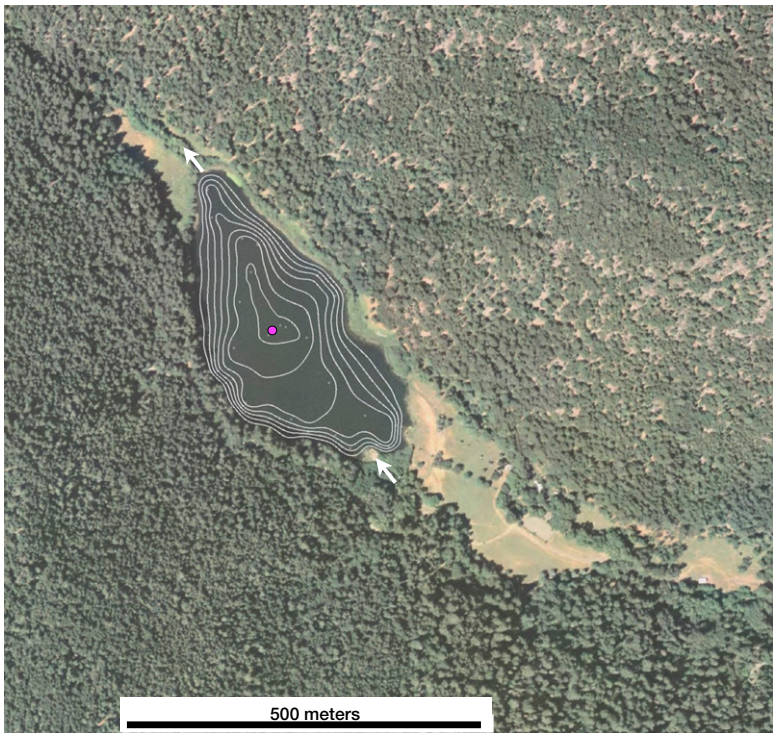

Fig. S3. Bathymetric map of USL, Jackson County, Oregon, superimposed on an aerial photograph. Isobath interval is 2 m, ranging from 2–14 m. Bathymetry was interpolated between depth soundings recorded by a global positioning system (Garmin GPS60cs). The inlet and outlet are indicated by white arrows. Core location is shown by a magenta circle. The estimated lake volume is 564,000 m^3.

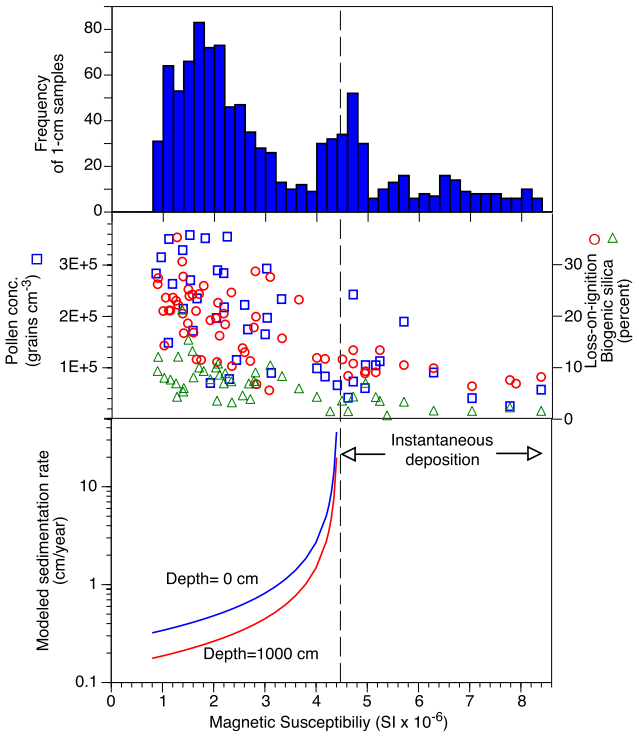

Fig. S4. Magnetic susceptibility, loss-on-ignition, and biogenic silica measurements from the USL sediment core. (*Top*) The frequency distribution of bulk core (5-cm diameter) magnetic susceptibility in SI units. Magnetic susceptibility was measured using a Sapphire Instruments ring meter at 1-cm intervals. (*Middle*) Sediment with high magnetic susceptibility has low pollen concentration (usually <10,000 grains cm^{-3}), low loss-on-ignition at 550 °C (usually <10%), and very low biogenic silica content (<3%). Biogenic silica was measured on samples spaced by 32 or 64 cm using a sodium carbonate extraction method (1). (*Bottom*) The sedimentation rate was modeled as a function of magnetic susceptibility, in which magnetic susceptibility is a proxy for the mixture of slowly deposited organic sediment and instantaneously deposited eroded inorganic sediment. This relationship differs slightly with core depth, as described in the main text.

1. Mortlock RA, Froelich PN (1989) A simple method for the rapid-determination of biogenic opal in pelagic marine sediments. *Deep-Sea Res A, Oceanogr Res Pap* 36:1415–1426.

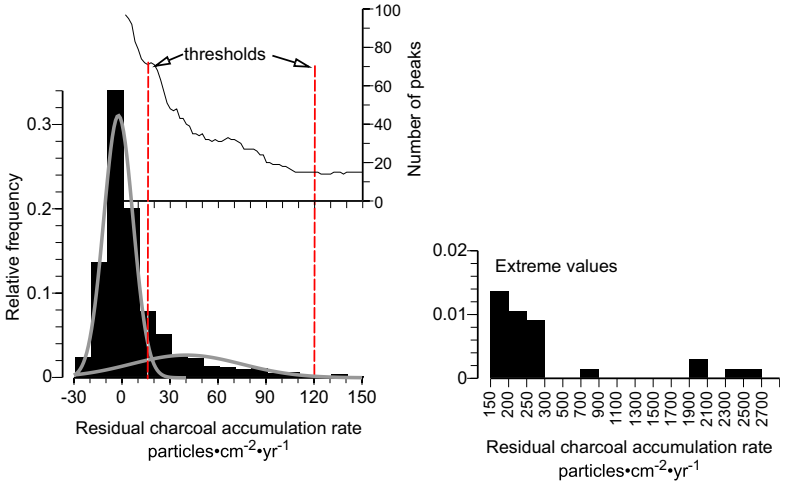

Fig. S5. The frequency distribution of charcoal accumulation rate values from the USL sediment core. The residual charcoal accumulation rate is the difference between observed and background charcoal accumulation rates. The fitted curves are calculated using a Gaussian mixture model in which three distributions were fit to the distribution of charcoal values (1). The right-most distribution, fit to the extreme values of the distribution, is not shown. Thresholds for identifying local fire events are shown by dashed red lines. Thresholds are placed where there is little sensitivity of the exact threshold level on the number of charcoal peaks identified and near the 99th percentile of the two fitted distributions. The upper ends of the fitted distributions represent distinct breaks in the distribution of charcoal values and are logical positions for thresholding.

1. Gavin DG, Hu FS, Lertzman K, Corbett P (2006) Weak climatic control of stand-scale fire history during the late Holocene. *Ecology* 87:1722–1732.

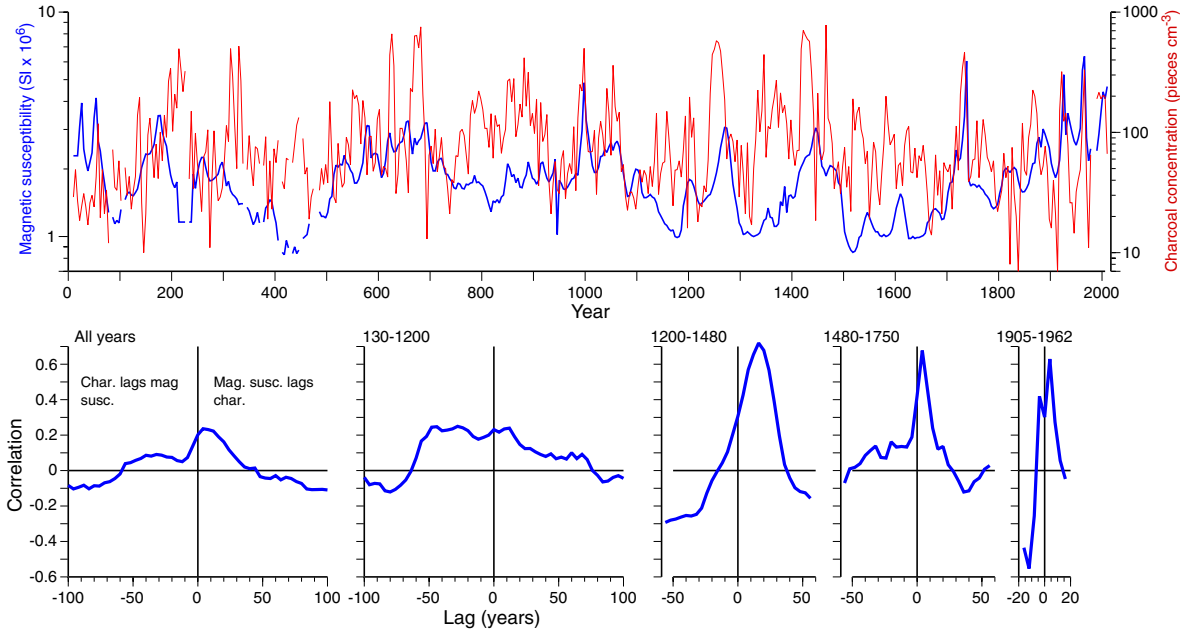

Fig. S6. Cross-correlograms show the charcoal concentration time series lags with respect to the magnetic susceptibility time series from the USL sediment core. Charcoal concentrations and magnetic susceptibility were interpolated to 2-y windows. Because magnetic susceptibility was used to infer sedimentation rates, charcoal concentration rather than charcoal accumulation rate was used for this analysis to avoid nonindependence between the two variables. Both time series were log-transformed before correlations were calculated. Cross-correlograms show that magnetic susceptibility lags with respect to charcoal concentration, indicating erosion following fire.

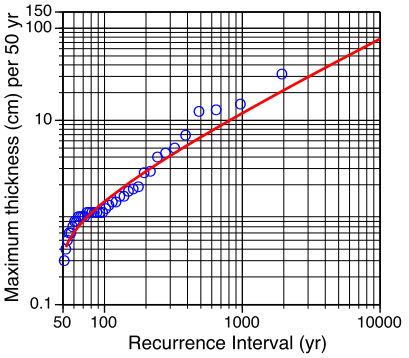

Fig. S7. Flood-frequency analysis applied to the minerogenic horizon chronology in the USL sediment core. The maximum minerogenic horizon thicknesses were determined in consecutive 50-y intervals for the 38 intervals from years A.D. 0–1900 (using data shown in Fig. 2*D* in the main text). The analysis shows the expected recurrence of minerogenic sediment layers over a range of thicknesses. The fitted curve was computed using the log Pearson type III distribution. This curve shows that the observed minerogenic layers during the 20th century, with thicknesses of 42 and 139 cm, have expected recurrence intervals of >4,000 and >10,000 y, respectively, based on the historical frequency–magnitude relationship.

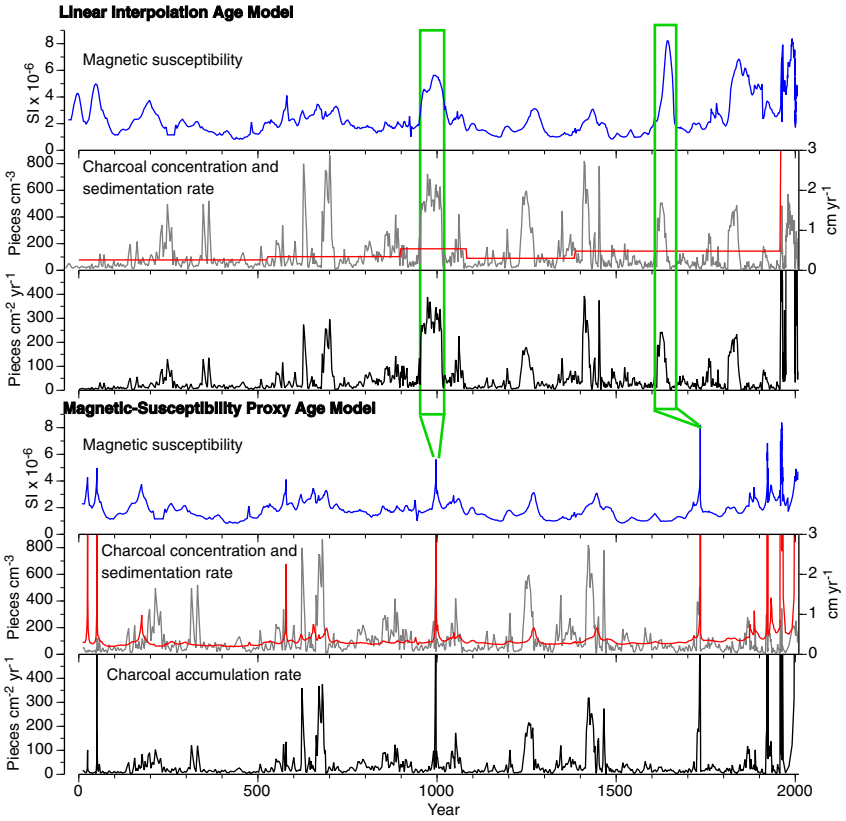

Fig. S8. Comparison between a linear interpolation model (*Upper*) and the magnetic susceptibility proxy age model used for this study (*Lower*). For each model, magnetic susceptibility (blue line), charcoal concentration (gray line), sedimentation rate (red line), and corresponding charcoal accumulation rates (CHAR values) (black line) are plotted for comparison. The interpolated age model fails to detect periods of higher sedimentation rates, resulting in higher CHAR values for those periods. Green rectangles show two examples of the effect of compressing periods of higher sedimentation rate as estimated by magnetic susceptibility values in our alternative model.

Table S1. Radiocarbon dates from the Upper Squaw Lake sediment core

Laboratory depth (cm)	No.	Material	^{14}C age ± 1σ	Calibrated 1σ range	Fitted age in Fig. 2
539.5	64498	Charred wood	615 ± 40	555–652	564
630.5	64497	Terrestrial plant macrofossil	980 ± 55	797–937	867
729	Beta-23617	Wood	1110 ± 40	971–1056	1051
856.5	64496	Bud scale	1610 ± 140	1357–1627	1422
952.5	64495	Douglas-fir needle	1870 ± 100	1695–1927	1791

AMS radiocarbon dates were obtained at the Woods Hole NOSAMS facility with the exception of sample at 729 cm from Beta Analytic, Inc. Radiocarbon dates were calibrated using CALIB Rev 5.0.2 (INTCAL04) (1, 2).

1. Reimer PJ, et al. (2004) IntCal04 terrestrial radiocarbon age calibration, 0-26 cal kyr BP. *Radiocarbon* 46:1029–1058.
2. Stuiver M, Reimer PJ (1993) Extended 14C database and revised CALIB radiocarbon calibration program. *Radiocarbon* 35:215–230.

Table S2. ^{137}Cs measurements from the Upper Squaw Lake sediment core

Upper depth (cm)	Lower depth (cm)	^{137}Cs activity ± 1 SD (DPM/g)
150	160	0.22 ± 0.07
180	190	0.30 ± 0.05
220	230	0.45 ± 0.08
250	260	0.34 ± 0.05
280	290	0.14 ± 0.07
350	360	0.06 ± 0.08

Measurements were made by Flett Research Inc., on bulk sediment sampled in 10-cm core segments. Very low activities [expressed as disintegrations per minute per gram (DPM/g)] are the result of a fast sedimentation rate.